Journal of Microscopy, Vol. 224, Pt 2 November 2006, pp. 197–202
Received 14 October 2005; accepted 24 May 2006

Investigation of dyed human hair fibres using apertureless near-field scanning optical microscopy

F. FORMANEK, Y. DE WILDE, G. S. LUENGO* & B. QUERLEUX*
Laboratoire d'Optique Physique, CNRS UPR A0005, Ecole Superieure de Physique et de Chimie Industrielles, 10 rue Vauquelin, 75005 Paris, France
**L'Oreal Recherche, Aulnay-sous-Bois, France*

Key words. Cuticle, dye, human hair, near-field optical microscopy.

Summary

We present the first studies of dyed human hair fibres performed with an apertureless scanning near-field optical microscope. Samples consisted of 5-μm-thick cross-sections, the hair fibres being bleached and then dyed before being cut. Hair dyed with two molecular probes diffusing deep inside the fibre or mainly spreading at its periphery were investigated at a wavelength of 655 nm. An optical resolution of about 50 nm was achieved, well below the diffraction limit; the images exhibited different optical contrasts in the cuticle region, depending on the nature of the dye. Our results suggest that the dye that remains confined at the hair periphery is mainly located at its surface and in the endocuticle.

Introduction

The cosmetics industry is very interested in understanding the penetration pathways of different elements into hair fibres in order to improve its knowledge of diffusion processes and to adapt the nature of its products to consumer demand. The penetration pathways into hair fibres are generally investigated using fluorescent dyes with classical optical microscopy, or confocal laser scanning microscopy (Corcuff *et al.*, 1993; Wortmann *et al.*, 1997; Swift, 2000). However, these techniques are limited by diffraction to about half the illumination wavelength, and cannot resolve inner cell structures. Near-field scanning optical microscopy was developed to break this resolution limit by using a nanometer-sized probe to reveal the evanescent field at the sample surface (Pohl *et al.*, 1984; Lewis *et al.*, 1984). In this way, the optical resolution is only limited by the size of the probe apex, i.e. its radius of curvature. Another advantage of near-field optics is possible imaging of chemical elemental composition (Knoll & Keilmann, 1999; Cricenti *et al.*, 2003), which is not feasible with an atomic force microscope. So far, most near-field studies on biological samples have been carried out using optical fibers (Betzig & Trautman, 1992; De Lange *et al.*, 2001; Lewis *et al.*, 2003). However, apertureless probes such as scattering metallic tips enable us to work over a broader spectral range and achieve better resolution (Inouye & Kawata, 1994; Zenhausern *et al.*, 1994; Gleyzes *et al.*, 1995; Formanek *et al.*, 2003). Despite several applications of atomic force microscopy to hair fibres (Luengo & Leroy, 2004; Breakspear *et al.*, 2005), the only near-field studies of human hair were, to our knowledge, performed using fluorescence detection by tapered optical fibers with metallic coatings (Kelch *et al.*, 2000).

Human hair fibres are generally 50–100 μm in diameter, and present three main structures (Zviak, 1986; Robbins, 2001) when observed in cross-section (Fig. 1a). The inner structure, with a diameter of about 5–10 μm, is called the medullary canal or medulla. The medulla, although not always present, is composed of cells separated by empty spaces and running along the longitudinal axis of the hair. The cortex, which constitutes the real core of the fibre, accounts for 90% of its total weight. It is made of elongated cortical cells (≈100 μm in length and ≈ 1–6 μm in diameter) aligned along the axis of the fibre, and contains semicrystalline substructures called macrofibrils (≈100–400 nm in diameter). Macrofibrils are rod-like structures consisting of fibrillar keratin embedded in an amorphous protein matrix. Keratin has the ability to crystallize in the form of an α-helical structure.

Cystine, serine, glycine and *N*-acetylserine are the main amino acids, and the chains are stabilized by a number of intermolecular and intramolecular interactions: electrostatic, van der Waals, hydrogen and covalent (disulphide) bonds. These units form hexagonal crystals called microfibrils (≈ 7.5 nm in diameter) or intermediate filaments. Fibrillar and matrix keratins build highly intricate structures that are strongly anisotropic, giving hair its unique mechanical properties: high rupture stress and elongation, high elastic modulus, and rapid and total recovery even at high deformation (Fraser *et al.*, 1976; Zviak, 1986; Briki *et al.*, 1998). The cortex also includes

Correspondence to: Y. De Wilde. Tel: +33 1 40794539; fax: +33 1 43362395; e-mail: dewilde@optique.espci.fr

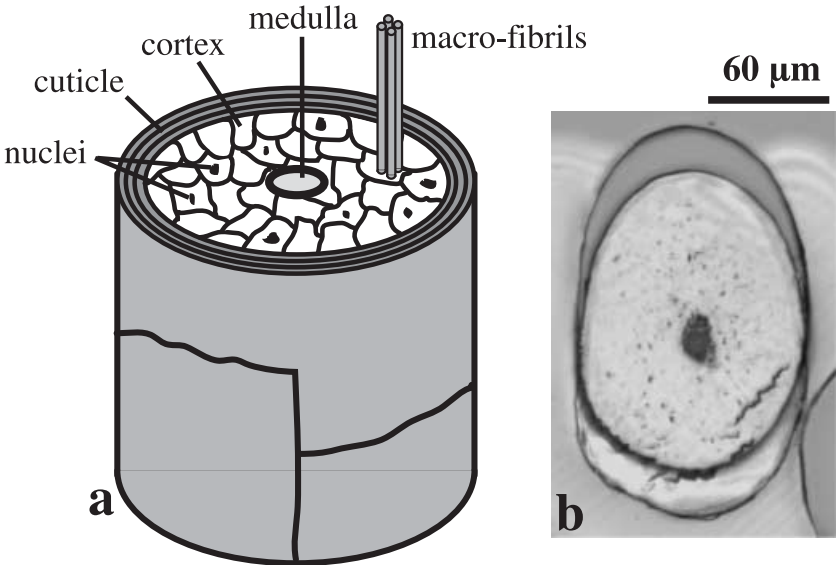

Fig. 1. (a) Main morphological structures present in a hair fibre. (b) Image of a microtomed cross-section of a hair fibre, obtained by classical optical microscopy.

melanin pigments, responsible for hair colour, as ovoid or spherical granules (≈ 200–800 nm in size). Hair thus appears as a true bio-nanocomposite.

The hair envelope protecting the cortex, which is called the cuticle, is composed of several (≈3–10) overlapping cells arranged in a layer about 1 µm thick (Swift, 1991, 1999). These cells are connected by lipid-rich intercellular material. Each overlapping cell is divided into three layers: the innermost endocuticle, the exocuticle, and the outermost epicuticle. The endocuticle, composed of cytoplasmatic and nuclear remnants, has a low cystine content (≈ 3%) and is considered to be the weakest component of the cuticle structure (torn scales usually break through this layer). The exocuticle is composed of a cystine-rich protein component; the part of the layer closest to the exocuticle is referred to as the A-layer. Its high cystine content suggests that the exocuticle is a highly cross-linked material, and is therefore more compact, which could account for its high mechanical resistance and water barrier behaviour. The final structure of the outermost layer of the cuticle is of especial interest, because the surface properties of hair depend on the physicochemical properties of this layer (Luengo & Leroy, 2004). The epicuticle membrane contains highly cross-linked protein (≈ 75%) and fatty acids (≈ 25%). Among the adsorbed fatty acids, 18-methyleicosanoic acid appears to be covalently joined via thioester linkages to the protein and is considered to play an important role in the physicochemical and tribological surface properties of hair (Negri *et al.*, 1996). However, further measurements need to be done to evaluate the accuracy of this representation, as well as the extent or ordering of this suspected monolayer: the degree of coverage on the scale structure, its dynamics in the presence of surfactants or various treatments, etc.

Thus, the optical methods used so far on human hair have achieved a resolution no better than a few hundred nanometers and involve a fluorescent dye, which complicates sample preparation and leads to photobleaching problems. The aim of this article is to demonstrate that a new technique, apertureless near-field scanning optical microscopy, is well adapted for the study of spatial variations of optical properties of human hair sections due to the presence of a dye, and can achieve a resolution as good as 50 nm. After presenting the technique, we show experimental images of human hair sections coloured with two different dyes with unprecedented resolution. This first investigation indicates that apertureless near-field scanning optical microscopy is particularly suitable for observing optical contrasts due to changes of dye concentration, with nanometer resolution.

Materials and methods

Samples

To demonstrate the capability of the instrument to provide different optical contrasts on near-field images of hair fibre, we prepared two sets of hair dyed with two molecular probes with different affinities for the fibre. The samples consisted of bleached white hair tresses immersed and stirred for 30 min at ambient temperature in a 2.5×10^{-3} m neutral solution (pH 7) of two red-absorbent molecular probes. Hairs were then cleaned by water rinsing, and finally dried. Subsequently, hairs were embedded in an LR White Medium grade resin. Thin cross-sections (≈ 5 µm thick) were obtained using a microtome diamond knife and deposited on a glass cover slip. The transparent resin is clearly visible on the outer parts of the image obtained with classical optical microscopy (Fig. 1b). Bleaching was performed by treating hair with a peroxide solution (hydrogen peroxide 15 vol., sodium peroxodisulphate 22% and ammonia 2.9%) for 50 min at 30 °C. Neutralization was performed in a 0.22% sodium thiosulphate solution for 30 min at 30 °C.

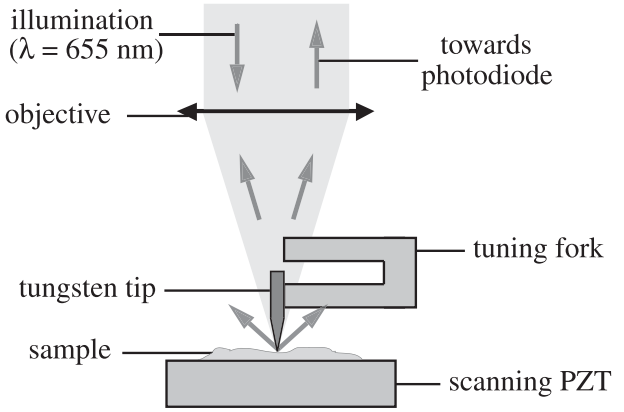

Fig. 2. Sketch of the experimental arrangement: a scanning near-field optical microscope based on a quartz tuning fork and operating in reflection mode. PZT, piezoelectric transducer.

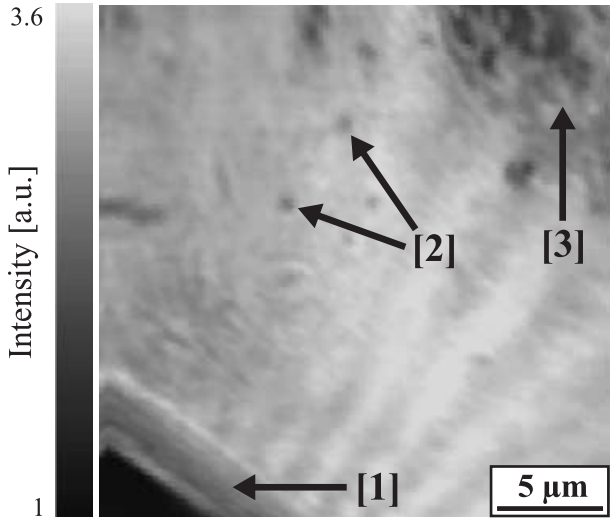

Fig. 3. Far-field optical image recorded at λ = 655 nm (without the tip) of a hair fibre cross-section on which a dye diffusing mainly at the surface was applied.

Methods

For the experiments, we used a home-made apertureless near-field scanning optical microscope in reflection mode (De Wilde *et al.*, 2003). The experimental setup is shown in Fig. 2. It is based on an atomic force microscope operating in tapping mode, combined with laser illumination of the tip. The probe consisted of a sharp metallic tungsten tip prepared by electrochemical etching (Oliva *et al.*, 1996). The role of the tip was to scatter the field located on the surface of the sample. Measurements of the scattered field were performed while the sample was scanned laterally under the tip. Our previous experiments (Formanek *et al.*, 2003) revealed that these tungsten tips typically have a radius of curvature of about 20 nm. Thus, the lateral resolution is strongly enhanced compared to what could be achieved with a conventional optical microscope. The tip was glued onto the lower arm of a quartz tuning fork (Karrai & Grober, 1995) and oscillated perpendicularly to the sample surface. The average distance between the tip and the sample surface was maintained at a constant value using electronic feedback of the tuning fork voltage. The total range of the piezoelectric transducer that controlled the tip height on the sample surface was 17 µm. This allowed us to follow important topographical variations that might occur, for instance, when the tip is moved from the substrate to the cuticle within the same scan, i.e. when the thickness of the hair section produces a step in the surface topography that is about 5 µm high. The beam from a laser diode (with wavelength 655 nm) was focused onto the sample through a high numerical aperture (NA) objective (50×, NA = 0.6) in order to illuminate the surface. The incident laser power used in the experiments was typically 10–20 mW, and the focalization spot was about 1 µm in diameter on the surface. The field scattered by the tip was collected by the same objective and sent towards a photodiode connected to a lock-in amplifier working at the tip oscillation frequency Ω or at its higher harmonics (2Ω and 3Ω). This technique allowed us to extract the weak contribution due to tip scattering from the background signal (Knoll & Keilmann, 2000; Formanek *et al.*, 2005).

Results and discussion

In order to better interpret the near-field optical images, we first obtained far-field images by removing the tip and the tuning fork. The beam from the laser diode (λ = 655 nm) was focused onto the hair surface through a high-NA objective (125×, NA = 0.8). Scattered light was collected by the same objective and modulated to a few hundreds of hertz using a mechanical chopper, and then focused with a lens onto a photodiode placed after a diaphragm. This diaphragm is mounted in the image plane of the sample, in such a way that only light scattered at the tip apex can reach the detector. The photodiode was connected to a lock-in amplifier working at the modulation frequency imposed by the chopper. The optical image was obtained by scanning the sample with a piezoelectric stage and recording the signal for each position, as in confocal laser scanning microscopy (Hadjur *et al.*, 2002). Figure 3 shows an $11 \times 11\ \mu m^2$ optical image thus obtained of a hair fibre on which a dye diffusing mainly at the surface level was applied. This image reveals different structures such as the cuticle (arrow 1), melanin pigments (arrow 2) and the medullar channel (arrow 3). However, the resolution, estimated to be about 400 nm, remained too low to resolve the inner structures of the cuticle and to study the penetration pathways of dyes.

Figure 4(a) shows a $10 \times 10\ \mu m^2$ topographical image of a hair fibre on which a dye diffusing deep inside the fibre was applied. Figure 4(b) shows the optical near-field image

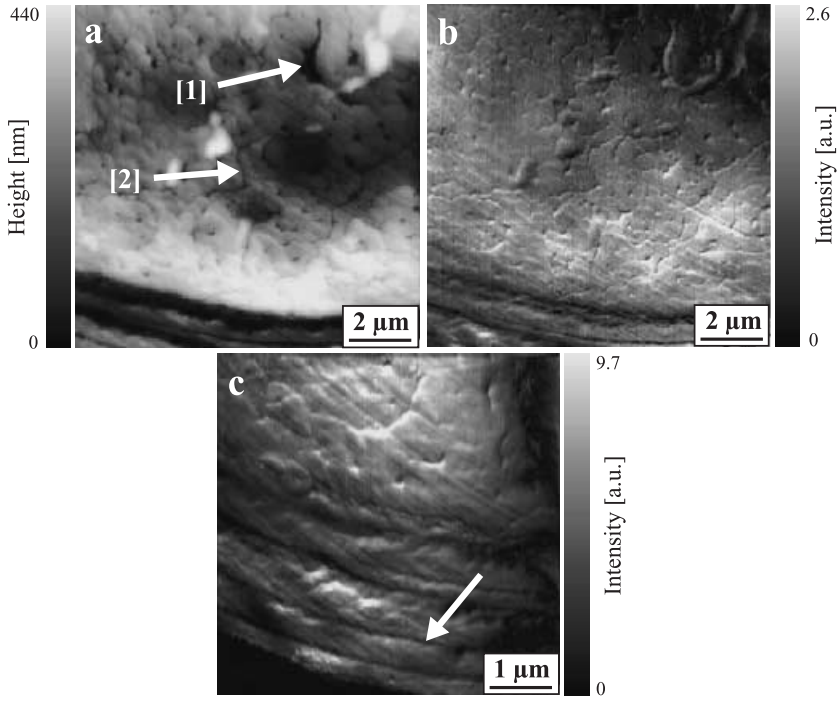

Fig. 4. Images of a hair fibre cross-section on which a dye diffusing deep inside the fibre was applied. (a) Topographical image and (b) corresponding near-field optical image recorded at $\lambda = 655$ nm. (c) Near-field optical image of a magnified view of the cuticle.

simultaneously recorded at 3Ω. Figure 4(c) is an optical near-field image of a magnified view of the cuticle (5.5×5.5 µm^2). The advantages of demodulating the optical signal at higher harmonics are that the interference effects can be reduced and the resolution slightly improved (Knoll & Keilmann, 2000). The near-field optical images clearly show better resolution than the far-field image. The topography reveals the remanence of nuclei (arrow 1) and borders (arrow 2) of cortical cells. The macrofibrils (≈ 100–400 nm in diameter) located inside the cortex explain the granular appearance of the hair body. Although such details are also visible on the optical image (Fig. 4b), the contrast is rather homogeneous over the whole cortex and the cuticle, as seen in natural hair fibre images (not shown here). However, Fig. 4(c) shows strong contrast at the outer part of each cuticle cell (indicated by the arrow). As the optical contrast follows the important topographical variations occurring at these precise positions, it may simply arise from a topographical artefact (Hecht *et al.*, 1997) rather than from spatial variations in dye concentration. One way to get rid of such artefacts would be to obtain constant height mode images, but it is not applicable for samples with important relief variations.

Figure 5(a) shows a 4.7×4.7 µm^2 topographical image of a hair fibre on which a dye diffusing mainly at the surface was applied. Figure 5(b) shows the optical near-field image simultaneously recorded at 2Ω. The optical resolution is estimated from a profile (Fig. 5c) to be about 50 nm. Here it is defined as the width of the smallest detail that can be observed in the image. The topographical image reveals parallel traces a few nanometres high, which are clearly visible on the cuticle (indicated by the arrow). Parallel traces of the same kind are also visible on the cortex region in Fig. 4. These traces are generally observed in atomic force microscopy measurements on microtome cuts of human hair (Luengo, unpublished data). As hair is a soft material, they are reminiscent of the traces resulting from sliding of the diamond knife at the surface of the hair section that occurs when performing the microtome cut. As they can be clearly distinguished from intrinsic hair structure, they do not hinder the interpretation of the near-field optical images.

The dark stripes (arrow 1) on the optical image show interferences (Formanek *et al.*, 2005) where the optical signal is equal to zero. Interferences are sometimes expected when the scan size is of the same order or larger than the wavelength of the laser illumination. Outside these interferences, the signal is almost homogeneous except in some bright regions (arrow 2) corresponding to the location of the intercellular material and/or the endocuticle. The external edge of the hair fibre (arrow 4) also presents a bright region. The optical contrast in the vicinity of these bright regions (Fig. 5b) is opposite to that observed in the surface topography (Fig. 5a), which rules out the possibility of a topographical artefact. Intermediate areas (arrow 3) including the exocuticle and the epicuticle appear with the same amount of signal as the cortex. This observation was reproduced in several experiments, i.e. with different tips and on different hair sections. The bright regions at the location of the intercellular material and/or the endocuticle, and at the external edge, have only been observed on hair coloured with a dye that mainly diffuses at the hair periphery, and never on natural hair or on hair coloured with a dye that

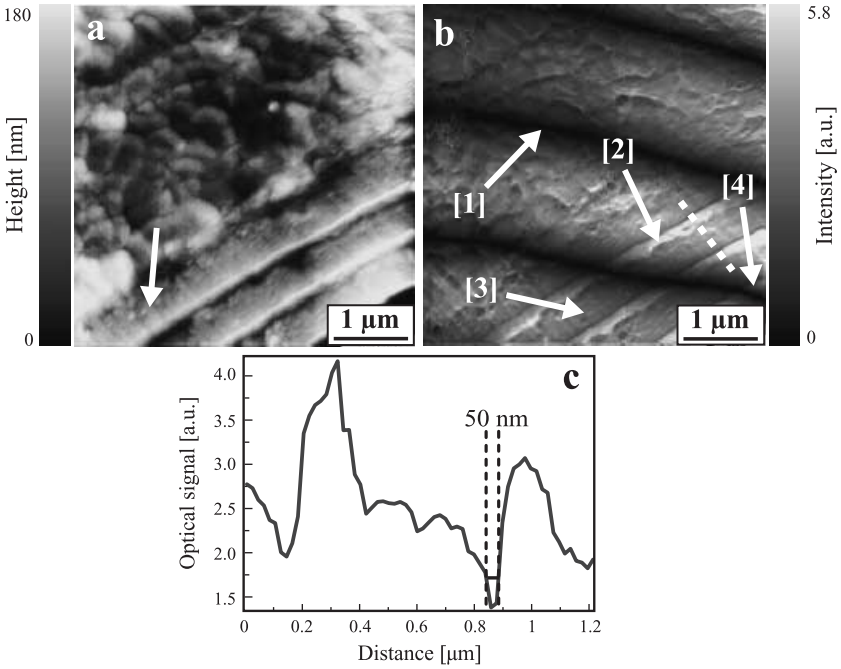

Fig. 5. (a) Topographical image and (b) corresponding near-field optical image of a hair fibre cross-section on which a dye diffusing mainly at the surface was applied, recorded at $\lambda = 655$ nm. (c) Profile of the dotted line visible in (b).

diffuses homogeneously. We therefore conclude that the bright regions correspond to zones with a higher dye concentration than the surrounding areas. From their shape and thickness, it is assumed that these bright regions correspond to the endocuticle and may include the intercellular material.

Using lock-in detection of the optical signal combined with an oscillatory movement of the tip in a direction z perpendicular to the sample surface provides information regarding the variation of the electromagnetic energy density ε along z. In a rough approximation, the lock-in signal demodulated at the fundamental tip frequency Ω is $S_\Omega \propto \partial\varepsilon/\partial z$, whereas the signals demodulated at higher harmonics are $S_{2\Omega} \propto \partial^2\varepsilon/\partial z^2$ and $S_{3\Omega} \propto \partial^3\varepsilon/\partial z^3$. Hence, an optical image recorded with an apertureless near-field scanning optical microscope cannot be quantitatively interpreted in simple terms. A quantitative study of spatial variations of dye concentration in human hair sections based on the contrast observed in apertureless near-field optical images would require a precise knowledge of the optical indices of the investigated dyes and of hair materials, the use of hair from the same batch coloured with different dyes, and the performance of tip-approach curves at various locations combined with theoretical modelling based on electrostatic dipole theory (Knoll & Keilmann, 2000). This is well beyond the scope of this article.

Discussion

The first studies of human hair fibres using an apertureless scanning near-field optical microscope are reported. Our optical images recorded at a wavelength of 655 nm show a resolution of about 50 nm, higher than that obtained with optical fibre probes. We were able to observe different optical contrasts on near-field images of hair fibres, depending on the nature of the applied dye. Whereas the dye diffusing deep inside the fibre gave no optical contrast, the dye diffusing mainly at the surface level showed that the major diffusion process seemed to occur in the cell membrane complex located between the outer cells of the cuticle and/or the endocuticle. With use of a slightly modified version of our setup, the imaging technique described here can be easily applied to biological systems in aqueous media. Preliminary steps in this direction have already been reported by some of us (Fragola *et al.*, 2004).

Acknowledgements

Part of this work (YDW, FF) was funded by the French Ministere de la Recherche, ACI Jeunes Chercheurs, project number 2039. The authors thank P. Barbarat, G. Madry, C. Hadjur and F. Leroy (L'Oreal) for preparing the samples and for their support. They are also grateful to L. Aigouy for fruitful discussions.

References

Betzig, E. & Trautman, J.K. (1992) Near-field optics: microscopy, spectroscopy, and surface modification beyond the diffraction limit. *Science*, **257**, 189–195.

Breakspear, S., Smith, J.R. & Luengo, G. (2005) Effect of the covalently linked fatty acid 18-MEA on the nanotribology of hairs outermost surface. *J. Struct. Biol.* **149**, 235–242.

Briki, F., Busson, B. & Doucet, J. (1998) Organization of microfibrils in keratin fibers studied by X-ray scattering: modeling using the paracrystal concept. *Biochim. Biophys. Acta*, **1429**, 57–68.

Corcuff, P., Gremillet, P., Jourlin, M., Duvault, Y., Leroy, F. & Leveque, J.L. (1993) 3D reconstruction of human hair by confocal microscopy. *J. Soc. Cosmet. Chem.* **44**, 1–12.

Cricenti, A., Generosi, R., Luce, M., *et al.* (2003) Chemically resolved imaging of biological cells and thin films by infrared scanning near-field optical microscopy. *Biophys. J.* **85**, 2705–2710.

De Lange, F., Cambi, A., Huijbens, R., *et al.* (2001) Cell biology beyond the diffraction limit: near-field scanning optical microscopy. *J. Cell. Sci.* **114**, 4153–4160.

De Wilde, Y., Formanek, F. & Aigouy, L. (2003) Apertureless near-field scanning optical microscope based on a quartz tuning fork. *Rev. Sci. Instrum.* **74**, 3889–3891.

Formanek, F., De Wilde, Y. & Aigouy, L. (2003) Imaging subwavelength holes using an apertureless near-field scanning optical microscope. *J. Appl. Phys.* **93**, 9548–9552.

Formanek, F., De Wilde, Y. & Aigouy, L. (2005) Analysis of the measured signals in apertureless near-field optical microscopy. *Ultramicroscopy*, **103**, 133–139.

Fragola, A., Aigouy, L., Mignotte, P.Y., Formanek, F. & De Wilde, Y. (2004) Apertureless scanning near-field fluorescence microscopy in liquids. *Ultramicroscopy*, **101**, 47–54.

Fraser, R.D., MacRae, T.P. & Suzuki, E. (1976) Structure of the alpha-keratin microfibril. *J. Mol. Biol.* **108**, 435–452.

Gleyzes, P., Boccara, A.C. & Bachelot, R. (1995) Near-field optical microscopy using a metallic vibrating tip. *Ultramicroscopy*, **57**, 318–322.

Hadjur, C., Daty, G., Madry, G. & Corcuff, P. (2002) Cosmetic assessment of the human hair by confocal microscopy. *Scanning*, **24**, 59–64.

Hecht, B., Bielefeldt, H., Inouye, Y., Pohl, D.W. & Novotny, L. (1997) Facts and artifacts in near-field optical microscopy. *J. Appl. Phys.* **81**, 2492–2498.

Inouye, Y. & Kawata, S. (1994) Near-field scanning optical microscope with a metallic probe tip. *Opt. Lett.* **19**, 159–161.

Karrai, K. & Grober, R.D. (1995) Piezoelectric tip-sample distance control for near field optical microscopes. *Appl. Phys. Lett.* **66**, 1842–1844.

Kelch, A., Wessel, S., Will, T., Hintze, U., Wepf, R. & Wiesendanger, R. (2000) Penetration pathways of fluorescent dyes in human hair fibres investigated by scanning near-field optical microscopy. *J. Microsc.* **200**, 179–186.

Knoll, B. & Keilmann, F. (1999) Near-field probing of vibrational absorption for chemical microscopy. *Nature*, **399**, 134–137.

Knoll, B. & Keilmann, F. (2000) Enhanced dielectric contrast in scattering-type scanning near-field optical microscopy. *Opt. Commun.* **182**, 321–328.

Lewis, A., Isaacson, M., Harootunian, A. & Muray, A. (1984) Development of a 500 Å spatial resolution light microscope. *Ultramicroscopy*, **13**, 227–231.

Lewis, A., Taha, H., Strinkovski, A., Manevitch, A., Khatchatouriants, A., Dekhter, R. & Ammann, E. (2003) Near-field optics: from subwavelength illumination to nanometric shadowing. *Nat. Biotechnol.* **21**, 1378–1386.

Luengo, G. & Leroy, F. (2004) The science of beauty at small scale. Applications of scanning probe methods on cosmetic science. *Applied Scanning Probe Methods* (ed. by B. Bhushan, H. Fuchs and S. Hosaka), pp. 363–386. Springer, Berlin.

Negri, A.P., Rankin, D.A., Nelson, W.G. & Rivett, D.E. (1996) Transmission electron microscope study of covalently bound fatty acids in the cell membranes of wool fibres. *Textile Res. J.* **66**, 491–495.

Oliva, A.I., Romero, A.G., Pena, J.L., Anguiano, E. & Aguilar, M. (1996) Electrochemical preparation of tungsten tips for a scanning tunneling microscope. *Rev. Sci. Instrum.* **67**, 1917–1921.

Pohl, D.W., Denk, W. & Lanz, M. (1984) Optical stethoscopy: image recording with resolution $\lambda/20$. *Appl. Phys. Lett.* **44**, 651–653.

Robbins, C.R. (2001) *Chemical and Physical Behavior of Human Hair*, 4th edn. Springer Verlag, New York.

Swift, J.A. (1991) Fine details on the surface of human hair. *Int. J. Cosmet. Sci.* **13**, 143–159.

Swift, J.A. (1999) Human hair cuticle: biologically conspired to the owner's advantage. *J. Cosmet. Sci.* **50**, 23–47.

Swift, J.A. (2000) Further comments on 'Pathways for aqueous diffusion in keratin fibers'. *Text. Res. J.* **70**, 277–278.

Wortmann, F.J., Wortmann, G. & Zahn, H. (1997) Pathways for dye diffusion in wool fibers. *Text. Res. J.* **67**, 720–724.

Zenhausern, F., O'Boyle, M.P. & Wickramasinghe, H.K. (1994) Apertureless near-field optical microscope. *Appl. Phys. Lett.* **65**, 1623–1625.

Zviak, C. (1986) *The Science of Hair Care*. Marcel Dekker, New York.